



Agilent EEsof EDA

Overview on 1.6-mW LC-tuned VCO Design for 2.4GHz in 0.18-um RF CMOS Technology

This document is owned by Agilent Technologies, but is no longer kept current and may contain obsolete or inaccurate references. We regret any inconvenience this may cause. For the latest information on Agilent's line of EEsof electronic design automation (EDA) products and services, please go to:

www.agilent.com/find/eesof

Design of a 1.6-mW LC-tuned VCO for 2.4GHz applications in 0.18-um RF CMOS technology

Stein Erik Weberg, RF Designer and
Bertel-Eivind Flaten, R&D Director,
Nordic VLSI, Norway

Abstract

A 2.4GHz fully integrated voltage-controlled oscillator has been designed in a 0.18-um RF CMOS process. Using only 1.2mA of current from a 1.3V power supply, the circuit shows a measured single-sideband phase noise of -117dBc/Hz at 1.0MHz offset frequency. The VCO can produce a GFSK-modulated output by adding a pair of small varactors in parallel to the resonance tank. The design of this VCO using the Agilent ADS harmonic balance and Momentum simulators will be described. The simulation results showing very good agreement with measurements will also be discussed.

1. Introduction

As CMOS process scaling goes further, CMOS realizations of transceiver front-ends become more and more attractive compared to bipolar solutions, also when considering power consumption. As market forces now drive total current consumption for wireless transceivers below 10mA, strict power constraints are imposed on all modules, including the VCO. It is therefore the task of the designer to design the most power-efficient VCO while fulfilling the phase-noise specification.

Several VCOs for 2.4GHz and above have already been presented ([4]-[9]), but for many of these designs the most important goal has been to minimize phase noise rather than minimizing power consumption.

This paper describes the design of a very low-power monolithic VCO intended for use in a 2.4GHz GFSK transmitter employing open-loop PLL direct VCO modulation. Other practical aspects of the design will be emphasized rather than deep theoretical treatments of phase noise, which has been covered in detail for this kind of oscillators in [1] and [2].

2. Specification

As this VCO is intended for use in an open-loop PLL modulation scheme (see Fig. 1), several requirements may be more strict compared to closed-loop operation. This is

especially true for phase noise, as the noise is no longer shaped by the PLL when the loop is opened. In addition, meeting the modulation index stability requirements may present a challenge.

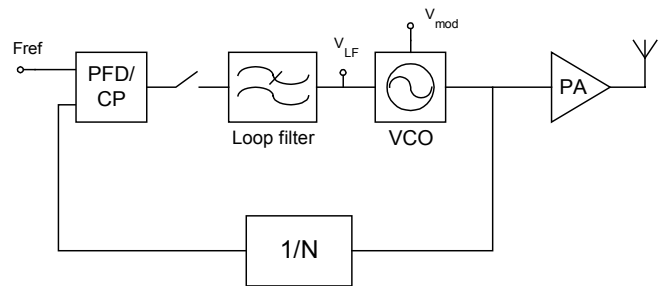


Figure 1 Simplified PLL modulator diagram showing reference frequency and modulating signal inputs

Phase Noise

For the application at hand, simulations show that adjacent channel transmitted power is not the limiting factor when it comes to phase noise. It is thus the modulated wave's signal-to-noise ratio (SNR) that sets the specification for oscillator phase noise. When modulating the VCO, the instantaneous output frequency will be the superposition of the modulation and the oscillator's internal noise signal, and the resulting average signal-to-noise ratio becomes

$$SNR \approx \frac{(\Delta f)^2 / 2}{2 \int_{f_1}^{f_2} f_m^2 L(f_m) df_m}, \quad (1)$$

assuming an IF equivalent noise bandwidth $B=2f_2$ in an imaginary noise free receiver. The choice of the lower integration bound f_1 is dependent on packet length in the transmission protocol. It is here assumed that noise at periods exceeding ten times the packet length do not contribute to the SNR. For the specification at hand [3], the maximum packet length is five slots, or 3.125 ms so $f_1=32\text{Hz}$.

It is worth mentioning that since CMOS oscillators exhibit substantial flicker noise, and since (in this case) the PLL is open during modulation, flicker noise will have quite a large

effect on total SNR, while it has only a marginal effect on the transmitted spectrum. To illustrate this point, Eq. 1 can be rearranged to plot SNR level curves in the $f_{\text{flk}}-L(1\text{MHz})$ plane, where f_{flk} is the value of the frequency offset f_m for which the up-converted flicker noise equals the up-converted white noise. It can be seen from the figure that if, for instance, a flicker noise knee of $f_{\text{flk}}=100\text{kHz}$ is achievable and the desired SNR is 30dB, the "white" phase noise at 1.0MHz will have to be around -115.5dBc/Hz , while -112.5dBc/Hz would be sufficient if no flicker noise was present. Still, for a relaxed specification such as Bluetooth we realize that one can tolerate quite high noise levels without sacrificing system performance. This, in turn, motivates an oscillator design where low phase noise is traded for low power.

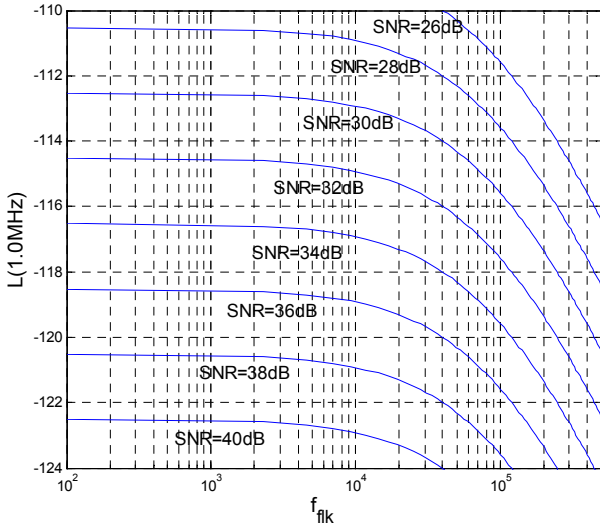


Figure 2 Curves of constant SNR assuming a noise bandwidth $B=2.0\text{MHz}$ and a peak deviation of $\Delta f=150\text{kHz}$

Frequency Deviation

The frequency deviation stability specification normally requires some sort of process compensation when the VCO is used for direct frequency modulation. This is a severe problem when modulation is performed by adding a voltage signal at the PLL loop filter node, as the large VCO tuning range is usually exploited for process compensating the center frequency of the VCO. This means that the VCO gain with respect to modulation (K_{MOD}) varies a lot over process, since the loop filter voltage may take on different values depending on other tank capacitance variations. In our case, however, the modulation is applied at another node with predefined, optimum bias conditions such that the nonlinear main varactor capacitance vs. voltage characteristic has no effect on deviation.

Now, deviation will still be somewhat dependent on the total capacitance in the tank. Assuming the inductance has little or no process variation, it can be shown that the deviation will only be dependent on channel number and the modulation varactor's capacitance variations itself. The inductor's parasitic capacitances will certainly vary a lot over process, but this will be compensated for by the tuning of the loop filter voltage until the correct channel frequency is reached. The dependence of deviation upon channel number, or equivalently, oscillation frequency is:

$$\begin{aligned} \Delta f &= \frac{1}{2\pi\sqrt{LC}} - \frac{1}{2\pi\sqrt{L(C+C_{\text{mod}})}} \\ &= f_0 \left[1 - \frac{1}{\sqrt{1+C_{\text{mod}}/C}} \right] = f_0 \left[1 - \frac{1}{\sqrt{1+C_{\text{mod}}L(2\pi f_0)^2}} \right] \quad (2) \\ &\approx 2\pi^2 f_0^3 C_{\text{mod}} L \end{aligned}$$

where the necessary additional capacitance C_{mod} is needed to create a deviation of Δf from center frequency f_0 . This known relationship can thus be compensated for by using a programmable gain at the VCO modulation input, leaving the modulation varactor itself as the only source for variation in frequency deviation.

3. Design

As both low flicker-noise up-conversion and low power consumption are crucial in the application at hand, the well-known topology of Fig. 3 is adopted.

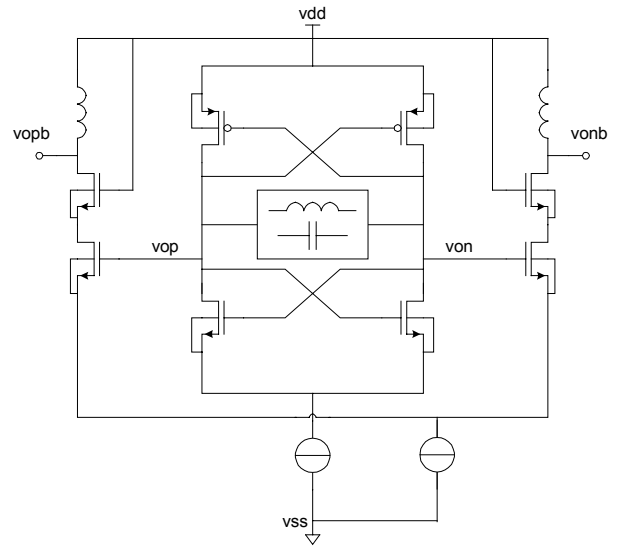


Figure 3 VCO core and output buffer

Resonance Tank

The resonance tank is shown in Fig. 4. It contains a 2.0nH planar, rectangular spiral inductor, a pair of MOS n-type varactors, a pair of plain MiM capacitors and two pairs (only one pair shown) of switched MiM capacitors to compensate for process variations. As the varactors have higher losses than MiM capacitors, the maximum size of the varactors is limited for phase noise reasons. This will, in turn, limit the VCO gain and therefore the maximum tuning range, but it will also reduce the oscillator's sensitivity to injected noise from other circuit components. At last, the tank also contains an extra set of very small varactors, suitable for analog FSK modulation. These should be so small that the noise from the pulse shaping filters do not affect carrier phase noise, but large enough so that their nonlinear C-V characteristic does not create intolerable spectral regrowth for the desired peak deviation.

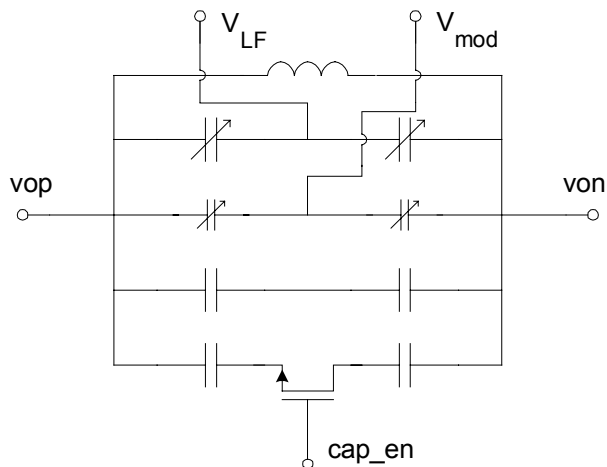


Figure 4 Resonance tank showing control (V_{LF}) and modulation (V_{mod}) inputs

Output buffer

As the oscillator frequency always will be subject to frequency pulling as power amplifier load impedance changes, it would be a good idea to use buffering with the maximum reverse isolation. As the oscillator is going to be capacitively loaded by a power amplifier, an inductively tuned differential cascode amplifier is used in this design. The simulated voltage gain is about 1dB using 0.4mA of current.

4. Experimental Results

The VCO was fabricated in a 6-metal-layer 0.18 μm CMOS process with extra thick top metallization. A section of the chip micrograph is shown in Fig. 5. The oscillator

core occupies less than 0.15mm² die area. The VCO output is sent through a -10dBm power amplifier before it goes off-chip for measurement.

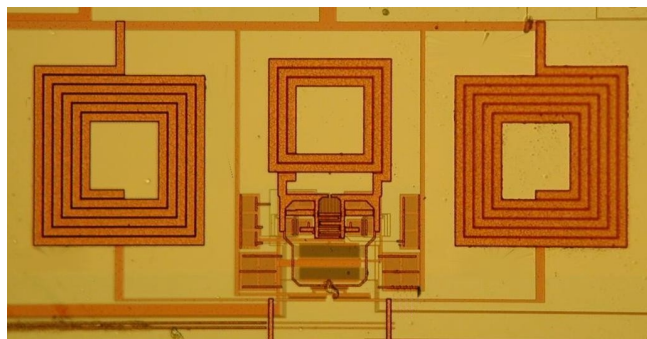


Figure 5 Section of die photo showing VCO (middle) and output buffer (bottom and sides)

Phase Noise

Phase noise was measured using the analog phase demodulation feature of an HP 89410 spectrum analyzer with RF extension. The measured spectrum can be seen in Fig. 6. Note that the instrument demodulates double-sideband, and that the single-sideband phase noise $L(f_m)$ may be obtained by subtracting 3dB from Fig. 6. The apparent flat part of the spectrum below 3kHz is due to the fact that the instrument operates with a resolution bandwidth of RBW=3kHz. This relatively high RBW means that the instrument is operating relatively close to its noise floor when measuring at 1.0MHz offset frequency. The measured flicker noise knee, f_{flk} , is about 150kHz for this design.

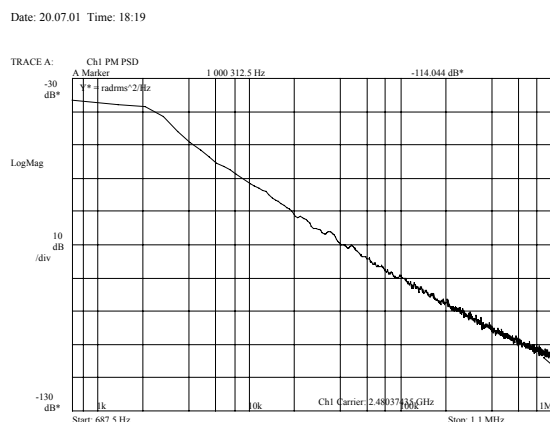


Figure 6 Measured Double-Sideband demodulated phase noise

If one is trying to quantify the "quality" of an oscillator, simply looking at the phase noise at one specific offset frequency is not enough. To be able to compare the oscillator phase noise to previously published designs, we

may use the PFN (*power-frequency-normalized*) figure of merit defined in [4],

$$PFN = 10 \log \left[\frac{kT}{P_{\text{sup}}} \left(\frac{f_0}{f_m} \right)^2 \right] - L(f_m) \quad (3)$$

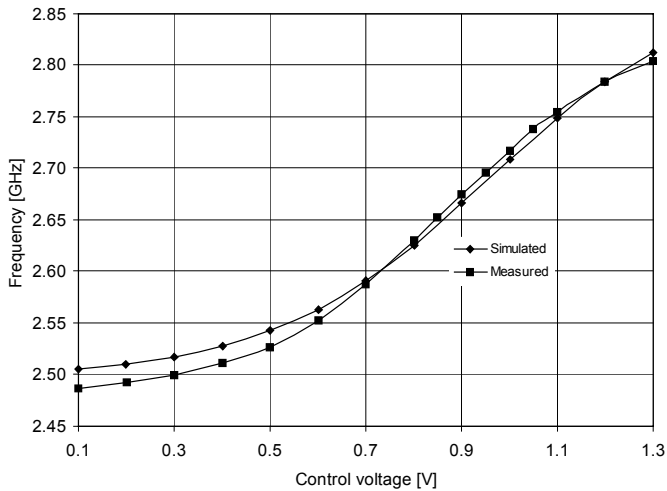
where $L(f_m)$ is expressed in dBc/Hz and a larger PFN corresponds to a better oscillator. This equation takes into account the physical phenomena that rule phase noise in oscillators, namely that phase noise is proportional both to the inverse of the dissipated power in the resonance tank and to the square of the f_0/f_m ratio. PFN for some previously published designs are shown in Table I. All designs are single-stage oscillators in CMOS technology except for [5], which is a quadrature LC-ring type of oscillator.

Table 1 Summary of CMOS oscillator properties

Ref	P_{sup} [mW]	f_0 [GHz]	f_m [MHz]	$L\{f_m\}$	PFN
Tiebout [5]	20.0	1.80	3.0	-143.0	11.7
This Work	1.56	2.48	1.0	-117.0	9.0
Hajimiri [1]	6.0	1.80	0.6	-121.0	8.8
De Ranter [6]	10.5	17.4	1.0	-108.0	8.6
Wang [7]	13.0	50.0	1.0	-99.0	7.8
Hegazi [8]	9.1	2.20	15.0	-148.0	7.3
Ham [4]	10.0	1.91	0.6	-121.0	7.1
De Muer [9]	34.2	2.00	0.6	-125.1	6.2

Tuning Range

The oscillator's tuning characteristic is shown in Fig.~5b. The frequency offset compared to the desired frequency range of 2.40-2.48GHz is due to poor accuracy of the inductor model at the time of design. Later simulations



using a field solver for the inductor show a 1.1 % accuracy for oscillator center frequency. The maximum gain occurs around 0.9V and is equal to $K_{VCO}=440$ MHz/V.

Figure 7 Measured and simulated tuning characteristic

Modulation Response

A digital synthesizer was used to create a Gaussian-filtered, random data signal with a bit rate of 1Mbit/s and BT=0.5. The 0.4V_{pp} voltage waveform was applied to the modulation input of the VCO, and the output spectrum and eye diagram can be examined in Fig. 8. The output spectrum is measured using max hold and RBW=100kHz.

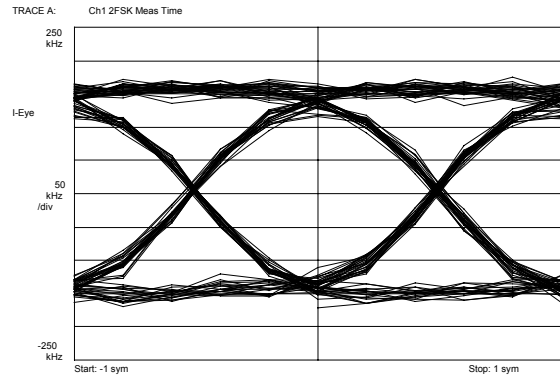


Figure 8 Measured modulation performance of the VCO: Eye diagram

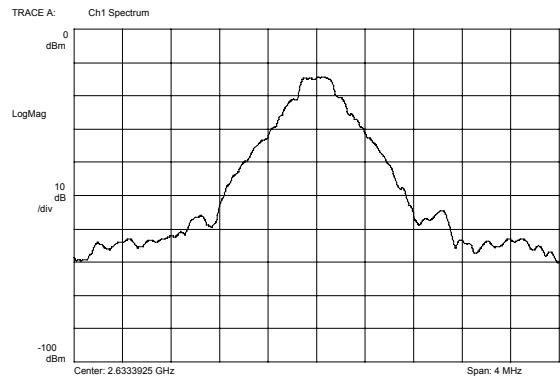


Figure 9 Measured modulation performance of the VCO: Output power spectrum

5. Conclusion

A 2.5GHz voltage-controlled oscillator has been designed in a 0.18- μm RF CMOS process. Using only 1.2mA of current from a 1.3V power supply, the circuit shows a measured single-sideband phase noise of -117dBc/Hz at 1.0MHz offset frequency.

When phase noise is normalized to power and frequency, the VCO shows excellent performance compared to other

recently reported designs. The VCO is also prepared for open-loop PLL GFSK modulation by adding an extra pair of small MOS varactors in parallel to the resonance tank. It is argued that this approach eliminates most of the process variation in frequency deviation. The modulation characteristics show excellent performance and Bluetooth compatibility.

Acknowledgements

The authors would like to thank all the people at the Wireless Communications department at Nordic VLSI ASA for valuable contributions to this work.

References

- [1] A. Hajimiri and T. H. Lee, "Design Issues in CMOS Differential LC Oscillators," *IEEE Journal of Solid-State Circuits*, vol. 34, pp. 717—724, May 1999.
- [2] A. Hajimiri and T. H. Lee, *The Design of Low Noise Oscillators*. Kluwer Academic Publishers, 1999.
- [3] Specification of the Bluetooth System, 1.1 ed., Feb. 2001.
- [4] D. Ham and A. Hajimiri, "Concepts and Methods in the Optimization of integrated LC VCOs," *IEEE Journal of Solid-State Circuits*, vol. 36, pp. 896—909, June 2001.
- [5] M. Tiebout, "Low-Power Low-Phase-Noise Differentially Tuned Quadrature VCO Design in Standard CMOS," *IEEE Journal of Solid-State Circuits*, vol. 36, pp. 1018—1024, July 2001.
- [6] C. De Ranter and M. Steyaert, "A 0.25 μ m CMOS 17GHzVCO," in *ISSCC Digest of Technical Papers*, pp. 370—371, Feb. 2001.
- [7] H. Wang, "A 50GHz VCO in 0.25 μ m CMOS," in *ISSCC Digest of Technical Papers*, pp. 372—373, Feb. 2001.
- [8] E. Hegazi, H. Sjöland, and A. Abidi, "A filtering Technique to Lower Oscillator Phase Noise," in *ISSCC Digest of Technical Papers*, pp.364—365, Feb.2001.
- [9] B. De Muer, M. Borremans, M. Steyaert, and G.L. Puma, "A2-GHz Low-Phase-Noise Integrated LC-VCO Set with Flicker-Noise Upconversion Minimization," *IEEE Journal of Solid-State Circuits*, vol. 35, pp. 1034—1038, July 2000.

Stein Erik Weberg was born in Trondheim, Norway in 1974. He received the M.Sc. degree in electronics engineering from the Norwegian University of Science and Technology in 1998.

Since 1999, he has been with Nordic VLSI ASA, Trondheim, Norway, where he is involved in the design of RF IC front-end circuits in CMOS and BiCMOS technology for the 433, 868/915 and 2400 MHz frequency bands.

Bertel-Eivind Flaten was born in Norway in 1960. He received the M.Sc. in electronic engineering from the Norwegian University of Science and Technology (NTNU) in 1984.

He worked for the Norwegian Defense Research Institute from 1985 to 1986. In 1995 he joined SINTEF, The Foundation for Scientific and Industrial Research at the Norwegian Institute of Technology, as a research scientist working with high speed/high frequency electronics. In 1994 he became research manager for the microelectronics division of SINTEF.

Mr. Flaten joined Nordic VLSI ASA in 1996 where he has been working with development of integrated RF transceivers for the 433, 868/915 and 2400 MHz frequency bands. His current position is R&D Director, Wireless Communication. He has also given lectures at the Norwegian University of Science and Technology.

For more information about Agilent EEs of EDA, visit:

www.agilent.com/find/eesof



Agilent Email Updates

www.agilent.com/find/emailupdates
Get the latest information on the products and applications you select.



Agilent Direct

www.agilent.com/find/agilentdirect
Quickly choose and use your test equipment solutions with confidence.

www.agilent.com

For more information on Agilent Technologies' products, applications or services, please contact your local Agilent office. The complete list is available at:

www.agilent.com/find/contactus

Americas

Canada	(877) 894-4414
Latin America	305 269 7500
United States	(800) 829-4444

Asia Pacific

Australia	1 800 629 485
China	800 810 0189
Hong Kong	800 938 693
India	1 800 112 929
Japan	0120 (421) 345
Korea	080 769 0800
Malaysia	1 800 888 848
Singapore	1 800 375 8100
Taiwan	0800 047 866
Thailand	1 800 226 008

Europe & Middle East

Austria	0820 87 44 11
Belgium	32 (0) 2 404 93 40
Denmark	45 70 13 15 15
Finland	358 (0) 10 855 2100
France	0825 010 700*
	*0.125 €/minute
Germany	01805 24 6333**
	**0.14 €/minute
Ireland	1890 924 204
Israel	972-3-9288-504/544
Italy	39 02 92 60 8484
Netherlands	31 (0) 20 547 2111
Spain	34 (91) 631 3300
Sweden	0200-88 22 55
Switzerland	0800 80 53 53
United Kingdom	44 (0) 118 9276201

Other European Countries:
www.agilent.com/find/contactus

Revised: March 27, 2008

Product specifications and descriptions in this document subject to change without notice.

© Agilent Technologies, Inc. 2008

Printed in USA, March 01, 2002
5989-8892EN



Agilent Technologies